

Prediction of plagioclase-melt equilibria in anhydrous silicate melts at 1-atm

Olivier Namur · Bernard Charlier ·
Michael J. Toplis · Jacqueline Vander Auwera

Received: 21 July 2010 / Accepted: 26 May 2011 / Published online: 14 June 2011
© Springer-Verlag 2011

Abstract Many models for plagioclase-melt equilibria have been proposed over the past 30 years, but the focus is increasingly on the effects of water content and pressure. However, many geological and petrological applications concern low pressure and low water systems, such as the differentiation of large terrestrial basaltic magma chambers, and lunar and asteroidal magmatism. There is, therefore, a justified need to quantify the influence of anhydrous liquid composition on the composition of equilibrium plagioclase at 1-atm. With this in mind, a database of over 500 experimentally determined plagioclase-liquid pairs has been created. The selected low pressure, anhydrous, experiments include both natural and synthetic liquids, whose compositions range from basalt to rhyolite. Four equations are proposed, derived from this data. The first is based on a

thermodynamically inspired formalism, explicitly integrating the effect of temperature. This equation uses free energies and activities of crystalline anorthite available from the literature. For the activity of anorthite in the liquid phase, it is found that current models of the activity of individual oxides are insufficient to account for the experimental results. We have therefore derived an empirical expression for the variation of anorthite activity in the liquid as a function of melt composition, based upon inversion of the experimental data. Using this expression allows the calculation of plagioclase composition with a relative error less than 10%. However, in light of the fact that temperature is not necessarily known for many petrological applications, an alternative set of T-independent equations is also proposed. For this entirely empirical approach, the database has been divided into three compositional groups, treated independently for regression purposes: mafic-ultramafic, alkali-rich mafic-ultramafic, and intermediate-felsic. This separation into distinct subgroups was found to be necessary to maintain errors below acceptable limits, but results across group boundaries were found to be comparable. Overall, 50% of plagioclase compositions are predicted to within 2% of the experimentally derived value, and 90% to within 5%, representing a significant improvement over existing models.

Communicated by T. L. Grove.

Electronic supplementary material The online version of this article (doi:10.1007/s00410-011-0662-z) contains supplementary material, which is available to authorized users.

O. Namur (✉) · B. Charlier · J. Vander Auwera
Department of Geology, University of Liège, Liège, Belgium
e-mail: obn21@cam.ac.uk

Present Address:

O. Namur
Department of Earth Sciences,
University of Cambridge, Cambridge, UK

Present Address:

B. Charlier
Department of Earth, Atmospheric and Planetary Sciences,
Massachusetts Institute of Technology, Cambridge, MA, USA

M. J. Toplis
IRAP (UMR5277 CNRS/Université Paul Sabatier),
Observatoire Midi-Pyrénées, 14, Av. E. Belin, Toulouse, France

Keywords Thermodynamics · Activity · Anorthite ·
Least-squares regression · Melt composition · Temperature

Introduction

Plagioclase, whose end-members are albite ($\text{NaAlSi}_3\text{O}_8$) and anorthite ($\text{CaAl}_2\text{Si}_2\text{O}_8$), crystallizes from an extremely diverse range of liquids (from basalt to rhyolite) over wide

ranges of temperature, pressure, and oxygen fugacity (fO_2). Plagioclase is one of the main rock-forming minerals of the Earth's continental crust and occurs in the Earth's mantle (Dijkstra et al. 2001). It is the major constituent of the lunar highlands (Wood et al. 1970; Hawke et al. 2003; Ohtake et al. 2009; Taylor 2009) and is found in many classes of meteorites (Rao et al. 1999; Renne 2000), on Mars, on Mercury, and in Vesta-sized planetesimals (Karner et al. 2004; Blewett et al. 2009). In other words, it is a ubiquitous component of rocky bodies in the solar system. As such, precise knowledge of the parameters controlling its composition is thus necessary to model many petrological processes associated with terrestrial and planetary differentiation.

Experimental studies on plagioclase-melt equilibria in complex silicate systems have shown that plagioclase composition essentially depends on (1) melt composition, especially water content (e.g., Housh and Luhr 1991; Sisson and Grove 1993; Panjasawatwong et al. 1995; Danyushevsky et al. 1997; Berndt et al. 2005; Takagi et al. 2005; Feig et al. 2006, 2010; Lange et al. 2009), (2) the temperature of crystallization (Kudo and Weill 1970; Mathez 1973; Lange et al. 2009), and (3) the pressure of crystallization (Lindsley 1970; Panjasawatwong et al. 1995; Fram and Longhi 1992; Longhi et al. 1993). Oxygen fugacity would not appear to significantly affect plagioclase composition (Glazner 1984; Toplis and Carroll 1995; Feig et al. 2010).

In recent years, several empirical or thermodynamic expressions of plagioclase-melt equilibria have been constructed with the aim of (1) predicting plagioclase composition as a function of equilibrium liquid composition or (2) estimating the conditions of crystallization, such as pressure and temperature. These predictive equations have been generally calibrated using experimental databases where plagioclase and liquid coexist in an equilibrium state. However, the strong interest in the effects of pressure and water content, motivated by the study of subduction related volcanism, has led many to understate the effect of anhydrous melt composition on plagioclase composition. Low-pressure anhydrous systems are numerous and important, such as layered intrusions emplaced at shallow levels in the crust (e.g., Skaergaard; Toplis and Carroll 1996; Thy et al. 2009), low-gravity extra-terrestrial bodies, such as the Moon and Vesta-sized planetesimals (Righter and Drake 1997), and potentially the late-stage evolution of magma oceans (Shearer et al. 2006). For this reason, we have compiled an extensive experimental database containing anhydrous melts equilibrated at 1-atm that cover the whole compositional range from basalt to rhyolite. This database has been used to assess the various models available in the literature and to propose new equations that allow prediction of the compositions of plagioclase (X_{An} = [molar Ca/(Ca + Na)]) as a function of melt composition \pm temperature.

Two calibration approaches have been used. In the first, we employ an equation inspired by the thermodynamic formalism describing liquid-mineral equilibria (e.g., Toplis 2005). However, we find that current thermodynamic data, in particular for the liquid phase, limit use of this approach. Furthermore, knowledge of the temperature at which equilibrium is expected is required, but this parameter is frequently unknown or poorly constrained in many petrological applications. For this reason, a second approach based upon purely empirical and T-independent equations is proposed. As detailed below, the suppression of the T-parameter decreases the ability to simultaneously account for the whole data set, but this situation has been remedied by subdividing the database into three groups of melt compositions (mafic magmas, alkali-rich mafic magmas, and intermediate to felsic magmas) that were regressed separately. This approach leads to a set of equations that predict plagioclase compositions with the same accuracy as the T-dependent thermodynamically derived model.

Experimental database

Selected experiments

The database initially contained 936 plagioclase-saturated anhydrous experiments equilibrated at 1-atm, compiled from 54 published experimental studies (Table A1; Supplementary Materials). Most of these studies were performed with natural or “complex” synthetic starting compositions (>8 oxide components), except those of Libourel et al. (1989), Shi and Libourel (1991), and Shi (1993) that are based on synthetic compositions from simplified systems (six or less oxide components). Most experiments were performed using the Pt wire loop technique, although a few were done in Mo, Fe, or AuPd capsules. Equilibrium temperatures ranged from 998 to 1,355°C, at oxygen fugacities ($\log fO_2$) from -0.68 (air) to -14.4 (Fig. A1; Suppl. Mat.). Plagioclase and melt were analyzed by electron microprobe in all studies.

In order to ensure that the selected plagioclase-melt pairs are in an equilibrium state, three filters have been applied to the experimental database: (1) only experiments with a proportion of quenched liquid higher than 50 wt% have been selected. When modal proportions are not reported, the proportion of melt has been calculated by least-squares regression using the algorithms of Stomer and Nicholls (1978); (2) only experiments with a run duration longer than 24 h have been retained, a duration typically considered sufficient for attainment of equilibrium in experiments with >50% liquid (Grove et al. 1982; Grove and Bryan 1983); (3) only experiments with microprobe totals between 98 and 101 wt% were selected.

Applying these criteria, the final database contains 530 plagioclase-melt pairs.

Magma types and compositions

Melts cover a compositional range from mafic (picrobasalt, basalt) to felsic (dacite, trachyte, rhyolite; Fig. 1, Table A2; Suppl. Mat.). Some experimental melts are highly enriched in alkalis (Na_2O and K_2O) and belong to the trachy-basalt, tephrite, phonotephrite, tephriphonolite, phonolite, and trachy-andesite magma types. As detailed in the following, for certain regressions of the experimental data, three different compositional groups were defined. The first group (298 experiments) is composed of mafic-ultramafic melts (basalt, picro-basalt, and tephrite). This group was limited to liquids with less than 52 wt% SiO_2 and 5 wt% $\text{Na}_2\text{O} + \text{K}_2\text{O}$ (Le Maitre 1989). Magmas from this first group span most of typical basaltic compositions from both the tholeiitic and the calc-alkaline series (Table A2; Suppl. Mat.). Experiments from this first group cover temperatures from 1,075 to 1,279°C and $\log f\text{O}_2$ ranging from -0.68 to -14.4 . The second group (69 experiments) consists of alkali-rich mafic-ultramafic melts (from tephrite to tephriphonolite; Table A2; Suppl. Mat.) with less than 52 wt% SiO_2 , but more than 5 wt% ($\text{Na}_2\text{O} + \text{K}_2\text{O}$). Melts from this group were equilibrated at temperatures in the range 1,080 to 1,273°C and $\log f\text{O}_2$ from -0.68 to -12.59 . The third group (163 experiments) contains intermediate to felsic melts with SiO_2 -contents higher than 52 wt%. They span the range from basaltic andesite to rhyolite in terms of SiO_2 -content and from basaltic andesite

to phonolite in terms of ($\text{Na}_2\text{O} + \text{K}_2\text{O}$)-content (Table A2; Suppl. Mat.). Experiments were performed at $\log f\text{O}_2$ between -0.68 and -13.3 and temperatures between 998 and 1,355°C.

Plagioclase composition

In the dataset, the plagioclase composition ($X_{\text{An}} = [\text{molar Ca}/(\text{Ca} + \text{Na} + \text{K})]$) ranges from 0.39 to 1.00 (Fig. A2; Suppl. Mat.): (1) $X_{\text{An}} = 0.48 - 1.00$ in the group of mafic-ultramafic melts; (2) $X_{\text{An}} = 0.44 - 0.89$ in the group of alkali-rich mafic melts; (3) $X_{\text{An}} = 0.39$ to 0.95 in the group of intermediate to felsic melts. The orthoclase content ($X_{\text{Or}} = [\text{molar K}/(\text{Ca} + \text{Na} + \text{K})]$) of the plagioclases is low (<0.06 ; Fig. A3; Suppl. Mat.).

Prediction of plagioclase composition

Previous calibrations

In the last decades, several models of plagioclase-melt equilibria have been proposed. Some of them allow calculation of the composition of plagioclase as a function of equilibrium melt composition, \pm other variables such as P and T (e.g., Weaver and Langmuir 1990; Grove et al. 1992; Panjasawatwong et al. 1995; Ghiorso and Sack 1995; Ghiorso et al. 2002; Putirka 2005; Takagi et al. 2005; Bédard 2006; Hamada and Fuji 2007). The accuracy of some of these models in predicting plagioclase compositions is tested here because they are built on convincing calibrations obtained by regressions of experimental datasets or detailed thermodynamic treatments. Predictive equations to calculate plagioclase compositions are given in the text, and information about calibration procedures is given in Table 1. The different models were tested with the filtered experimental database compiled for this study. Results of this investigation are listed in Table 1 and shown in Fig. A4 (Suppl. Mat.).

Model of Weaver and Langmuir (1990)

This model was designed to predict mineral (olivine, clinopyroxene, and plagioclase)-melt equilibria using intensive parameters such as melt composition and temperature. For predicting plagioclase composition, the model is based on the recasting of the melt composition in two components (NaAlO_2 and CaAl_2O_4), which are involved in the plagioclase solid solution. Based on thermodynamic modeling, the partition coefficients of NaAlO_2 and CaAl_2O_4 components between plagioclase and melt have been expressed as follows:

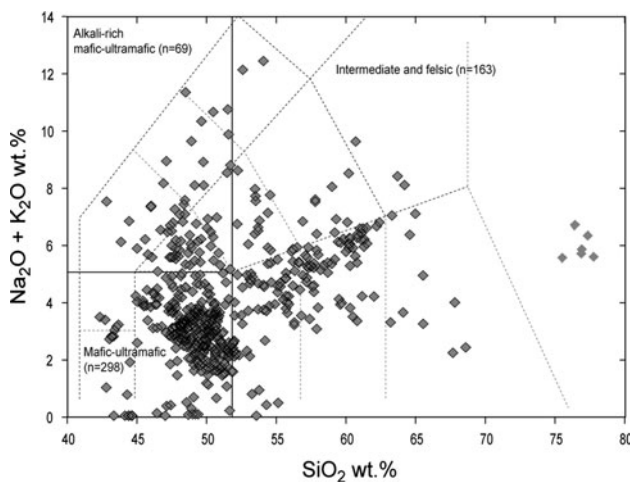


Fig. 1 Summary of experimental melt compositions ($n = 530$) used in calibration databases. The total alkali silica classification diagram is after Le Maitre (1989). For empirical predictive models, the database was divided into three groups of melt compositions: mafic-ultramafic, alkali-rich mafic-ultramafic, and intermediate to felsic magmas

Table 1 Synthesis of previous calibrations for prediction of plagioclase composition

Reference	Model type	Calibration				Test of the model										
		n^a	P (atm)	T (°C)	Melt comp. (SiO ₂ wt%)	H ₂ O (wt%)	Plag. comp. (An mol)	-LogfO ₂	Regression slope	Regression intercept	r^2	Delta anorthite	$1\sigma^d$	$\pm 5\%^e$	$\pm 10\%^f$	
Weaver and Langmuir (1990)	Theoretical thermodynamic model	–	–	–	–	–	–	–	0.79	0.13	0.65	0.35	0.25	0.057	62	83
Grove et al. (1992)	LSR	171	1–27000	1131–1420	43–60	–	0.45–0.80	7.93–9.40	0.62	0.28	0.66	0.30	0.35	0.050	58	84
Panjasawatwong et al. (1995)	LSR	39	5000–10000	980–1320	44–56	0.0–5.0	0.33–0.48		0.75	0.20	0.68	0.30	0.25	0.044	46	81
Melts/pMelts	Thermodynamics + LSR	>2500	1–105000	670–1700	<45–75	0.0–15.7	0.09–0.98	0–17.28	0.89	0.07	0.72	0.40	0.25	0.047	59	86
Putirka (2005)	LSR	306	1–20000	850–1350	42–73	0.0–7.0	0.40–0.95	7.74–12.86	1.25	–0.12	0.78	0.25	0.50	0.070	40	75
Takagi et al. (2005)	LSR	15	1000–5000	1100–1250	54–60	0.3–4.9	0.71–0.89	5.21–6.56	0.39	0.51	0.24	0.35	0.35	0.090	28	51
Bédard (2006)	LSR	988	1–30000	730–1430	42–76	0.0–6.0	0.10–1.00	7.00–16.00	0.24	0.49	0.39	0.5	0.2	0.073	42	75
Hamada and Fujii (2007)	Thermodynamics + LSR	55	1000–2700	1050–1260	50–58	0.0–4.7	0.71–0.94	7.09–9.61	0.93	0.01	0.64	0.45	0.15	0.061	62	84

^a n number of experiments used in the calibration database

^{b,c} Maximum negative and positive errors of the models (An mol; predicted–An mol; observed)

^d 1σ standard deviation of the errors of regression taken in absolute value

^e Percentage of the data with errors in the interval between –4 and +4%

^f Percentage of the data with errors in the interval between –10% and +10%; LSR Least square regression

$$\log K_d = \frac{a}{T(K)} + b \quad (1)$$

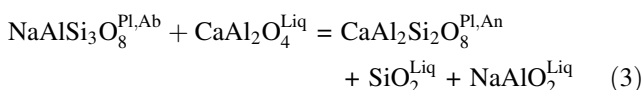
with a being a constant and b being a constant multiplied by the melt ratio $\text{CaAl}_2\text{O}_4/(\text{CaAl}_2\text{O}_4 + \text{NaAlO}_2)$. The An-content of plagioclase can then be calculated as follows:

$$X_{\text{An}} = \frac{K_d^{\text{CaAl}_2\text{O}_4}}{K_d^{\text{CaAl}_2\text{O}_4} + K_d^{\text{NaAlO}_2}} \quad (2)$$

Results of testing of Eq. 2 are presented in Table 1 and in Fig. A4a-b (Suppl. Mat.).

Model of Grove et al. (1992)

This model was originally designed to determine the composition of plagioclases crystallizing during the differentiation of mid-ocean ridge basalts (MORB). It is based on an expression of the equilibrium between plagioclase and melt which is represented by:



The model predicts the composition of plagioclase as a function of pressure and melt compositional variables (e.g., albite, anorthite, orthoclase) calculated following the equations of Bottinga and Weill (1972). The general form of the equation is given by:

$$X_{\text{An}} = \frac{A}{(1 + A)} \quad (4)$$

where A is defined as follows:

$$A = \frac{X_{\text{CaAl}_2\text{O}_4}}{X_{\text{NaAlO}_2} + X_{\text{SiO}_2} - X_{\text{NaAlO}_2}^2 - d(X_{\text{KAlO}_2})^2} \exp(a - bP(\text{Kbar}) - c) \quad (5)$$

where a , b , c , and d are regression coefficients that were fitted by multiple least-squares analysis. Results of testing of Eq. 4 are presented in Table 1 and in Fig. A4c-d (Suppl. Mat.).

Model of Panjasawatwong et al. (1995)

Panjasawatwong et al. (1995) have undertaken a detailed experimental study that was aimed at understanding the influence of melt composition on the origin of plagioclase with high An-content. They proposed an equation predicting the composition of plagioclase as a function of melt components, pressure, and temperature of crystallization, with the following general form:

$$X_{\text{An}} = \frac{1}{100} \left[\frac{a}{T(K)} + b + c \frac{P(\text{kbar})}{T(K)} + d \ln(\text{Ca}\#_{\text{melt}}) + e \ln(\text{Al}\#_{\text{melt}}) \right] \quad (6)$$

With $\text{Ca}\#_{\text{melt}}$ and $\text{Al}\#_{\text{melt}}$ being cationic $\text{Ca}/(\text{Ca} + \text{Na})$ and $\text{Al}/(\text{Al} + \text{Si})$ ratios, respectively. Results of testing of Eq. 6 are presented in Table 1 and in Fig. A4e-f (Suppl. Mat.).

Model of MELTS/pMELTS (Ghiorso and Sack 1995; Ghiorso et al. 2002)

MELTS/pMELTS is a thermodynamic model for twelve-component silicate liquids developed by Ghiorso and Sack (1995) and Ghiorso et al. (2002) in order to simulate igneous processes such as fractional and equilibrium crystallizations. Phase equilibria between melt and a particular crystalline phase can be obtained when liquid composition, $f\text{O}_2$, and pressure or temperature are given as input data. Calculations are performed by minimization of the appropriate thermodynamic potential (Ghiorso and Sack 1995). In this study, the MELTS/pMELTS algorithm was tested by introducing melt composition, pressure, and $f\text{O}_2$ as input data. To test the accuracy of the MELTS/pMELTS model in calculating plagioclase compositions, we have used the plagioclase An-content given by MELTS/pMELTS at the predicted-temperature of plagioclase saturation (Table 1; Fig. A4 g-h; Suppl. Mat.).

Model of Putirka (2005)

This model was designed for determining both the plagioclase composition and the temperature of crystallization as functions of melt composition and pressure. Predictive equations were obtained by least-squares multiple linear regression of experimental datasets. The equation for calculating plagioclase composition has the following general form:

$$\ln X_{\text{An}} = a + b \frac{P(\text{kbar})}{T(K)} + \frac{c}{T(K)} + \sum d_i Y_i \quad (7)$$

where a , b , c , and d are fitted terms and where Y_i are melt components or ratios of them. Results of testing of eq. 7 are presented in Table 1 and in Fig. A4i-j (Suppl. Mat.).

Model of Takagi et al. (2005)

Takagi et al. (2005) have performed a detailed experimental study in order to understand the origin of plagioclases with high An-content crystallizing from low-alkali hydrous tholeiitic basalts. Based on their experiments, these authors proposed an equation allowing to predict the composition of plagioclase as a function of the melt composition as well as the pressure and the temperature of crystallization:

$$\ln K_d^{\text{Ca-Na}} = \frac{a}{T(K)} + b + c \frac{P(\text{atm})}{T(K)} + d \text{H}_2\text{O}(\text{wt.}\%) \quad (8)$$

where a , b , c , and d are parameters fitted through multiple least-squares linear regression. Eq. 8 was initially designed for calculating the composition of plagioclase crystallizing from a hydrous melt. However, it can theoretically be solved for anhydrous systems by setting the d parameter to 0. Results of Eq. 8 are presented in Table 1 and in Fig. A4 k-l (Suppl. Mat.).

Model of Bédard (2006)

This model allows predicting the An-content of plagioclase as a function of melt composition, pressure and temperature following an equation with the following general form:

$$X_{\text{An}} = a + bT(^{\circ}\text{C}) + cP(\text{GPa}) + d\text{H}_2\text{O}(\text{wt.}\%) + e \ln \text{MgO}(\text{wt.}\%) \quad (9)$$

The parameters a , b , c , d , and e were empirically fitted by least-squares regression of natural and experimental datasets. Results of testing of Eq. 9 are presented in Table 1 and in Fig. A4 m–n (Suppl. Mat.).

Model of Hamada and Fuji (2007)

This model was initially designed to predict the composition of plagioclases crystallizing from tholeiitic magmas. It has the following general form:

$$\ln K_d^{\text{Ca-Na}} = \frac{a}{T(K)} + b \frac{P(\text{GPa})}{T(K)} + c \ln(Y_i) \quad (10)$$

where Y_i is a ratio of melt components (in wt%). The parameters a , b , and c are constant coefficients that were fitted by least-squares regression of an experimental dataset. Results are presented in Table 1 and in Fig. A4o-p (Suppl. Mat.).

Summary of previous calibrations

Based upon the comparison of modeled and observed plagioclase compositions (Table 1; Fig. A4; Suppl. Mat.), it is of note that all models tested predict some plagioclase compositions with significant errors ($1\sigma = 0.044 - 0.090$). Different causes can be identified to account for these errors: (1) some models were calibrated using databases containing a low number of experiments, with liquids covering a narrow compositional range; (2) many of these models were calibrated on the basis of experiments covering a significant range of pressure and melt water content. These two variables have a notable effect on plagioclase composition (Longhi et al. 1993; Lange et al. 2009), but their incorporation into predictive models tends

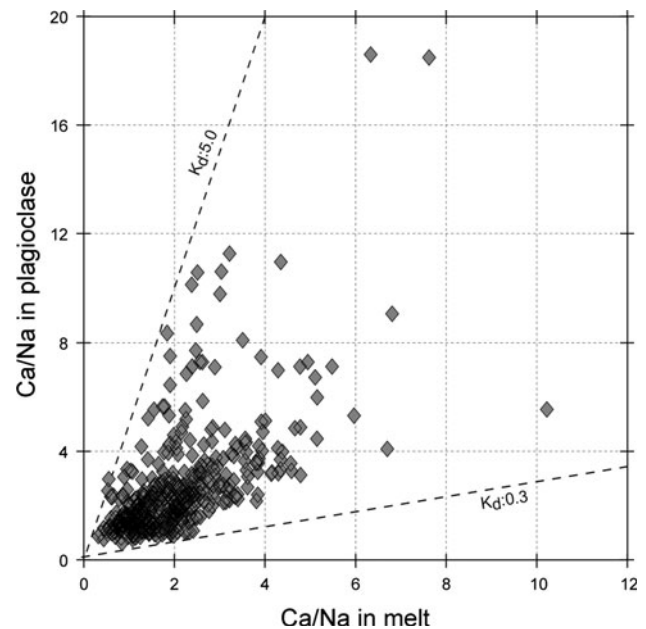


Fig. 2 Binary variation of Ca/Na ratios in plagioclases vs Ca/Na ratios in equilibrium melts. Representative points of some experiments from the database (with Ca/Na ratios higher than 20) are not plotted in order to conserve relatively narrow scales for X and Y axes

to attenuate the role of anhydrous liquid composition, leading to lower accuracy when predicting plagioclase compositions in such systems.

In light of these results, we will specifically concentrate on anhydrous melts experimentally equilibrated at 1-atm (1) to identify the melt compositional parameters that control composition of equilibrium plagioclase and (2) to calibrate new equations allowing the calculation of the An-content of plagioclase.

Predictive models of plagioclase-melt equilibria: general approach

The plagioclase solid solution is defined by the Ca/Na ratio, varying from the anorthite to the albite end-members. The Al/Si ratio varies in a complementary manner to maintain charge balance. To a first approximation, the composition of plagioclase may be expected to be simply related to the Ca/Na ratio of the melt in equilibrium with it, assuming that concentrations of Al and Si are not limiting. However, for our database, a plot of experimentally determined Ca/Na in liquid and plagioclase shows that no clear linear relation exists between these ratios (Fig. 2). The reasons for this are that the composition of a plagioclase crystallizing from a liquid depends on temperature, not to mention that the chemical potentials of Na, Ca, Al, and Si may all be complex functions of liquid composition: μ_1, \dots, μ_n , with $\mu > 10$ (Kudo and Weill 1970; Fram and Longhi 1992; Lange et al.

2009). We thus explored a thermodynamically derived model for the plagioclase-melt exchange reaction and then propose empirical T-independent models.

Thermodynamically derived model

Theoretical background

The relevance of thermodynamics in rationalizing plagioclase-melt equilibria has been recognized since the pioneering work of Bowen (1913) on the albite-anorthite system, and many subsequent studies have extended this approach (e.g., Kudo and Weill 1970; Henry et al. 1982; Glazner 1984; Elkins and Grove 1990; Holland and Powell 1992). The basic tenet of this approach is the equivalence of chemical potentials in coexisting phases at equilibrium. Considering the equilibrium between crystalline plagioclase and a silicate liquid, it may be written that:

$$\mu_i^{\text{Sol}} = \mu_i^{\text{Liq}} \tag{11}$$

where μ_i is the chemical potential of component i (albite: $\text{NaAlSi}_3\text{O}_8$, or anorthite: $\text{CaAl}_2\text{Si}_2\text{O}_8$ in this case). In detail, the chemical potential is represented by:

$$\mu_i^j = G_{(T)}^i + RT \ln(a_i^j) \tag{12}$$

where $G_{(T)}^i$ is the Gibbs free energy of the pure component i at the temperature T , R is the gas constant ($\text{J.K}^{-1}.\text{mol}^{-1}$) and a_i^j is the activity of component i in phase j . Thermodynamic activities may be related to molar concentrations (X_i^j) through the relation:

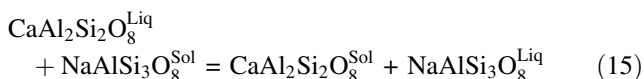
$$a_i^j = X_i^j \cdot \gamma_i^j \tag{13}$$

where γ_i^j is the activity coefficient of component i in phase j .

Combining Eqs. 11 and 12, it may be shown that the free energy of fusion (i.e., the difference, Δ , between the Gibbs free energy of liquid and crystal of the same composition at temperature T : ΔG^{fusion}) may be related to solid and liquid activities through the equation:

$$\frac{\Delta G_{i,(T)}^{\text{fusion}}}{RT} = \ln K_{\text{eq}} = \ln a_i^{\text{Sol}} - \ln a_i^{\text{Liq}} \tag{14}$$

Equation 14 can be applied directly for each individual component (albite or anorthite), or alternatively an exchange reaction can be written:



for which combination of Eqs. 14 and 15 leads to the relation:

$$\frac{\Delta G_{\text{An},(T)}^{\text{fusion}} - \Delta G_{\text{Ab},(T)}^{\text{fusion}}}{RT} = \ln \left(\frac{a_{\text{An}}^{\text{Sol}}}{a_{\text{Ab}}^{\text{Sol}}} \right) - \ln \left(\frac{a_{\text{An}}^{\text{Liq}}}{a_{\text{Ab}}^{\text{Liq}}} \right) \tag{16}$$

Equations 14 and 16 illustrate that the composition of equilibrium plagioclase is a function of temperature, T , and the composition of the melt that controls the terms a_i^{Liq} . As illustrated by the case of olivine (Toplis 2005), the temperature dependence of the terms on the left-hand side of Eq. 16 is attenuated when an exchange reaction such as Eq. 15 is considered.

Using the experimental database and standard-state thermodynamic data for albite and anorthite, we begin by calculating the $\Delta G/RT$ parameter (left-hand side of Eq. 16) as well as the activities of plagioclase components in the solid phase ($a_{\text{An}}^{\text{Sol}}$ and $a_{\text{Ab}}^{\text{Sol}}$, first term on the right-hand side of Eq. 16; see below). When combined with the experimental database, these terms allow the calculation of the activities of plagioclase components in the liquid phase ($a_{\text{An}}^{\text{Liq}}$ and $a_{\text{Ab}}^{\text{Liq}}$; second term on the right-hand side of Eq. 16), which may then be considered as a function of melt composition.

Thermodynamics of end-member components

The Gibbs free energy of fusion of component i at 1-atm is defined as follows:

$$\Delta G_{i,(T)}^{\text{fusion}} = \Delta H_{i,(T)}^{\text{fusion}} - T \Delta S_{i,(T)}^{\text{fusion}} \tag{17}$$

where Δ corresponds to the difference between liquid and solid, H is enthalpy and S is entropy of the system. At the melting temperature (T_m) of pure component i , $\Delta G^{\text{fusion}} = 0$, such that:

$$\Delta S_{i,T_m}^{\text{fusion}} = \frac{\Delta H_{i,T_m}^{\text{fusion}}}{T_m} \tag{18}$$

ΔH^{fusion} and ΔS^{fusion} are both functions of temperature and the complete expression describing the Gibbs free energy of fusion for the exchange of the component i between a crystalline phase and a melt is:

$$\Delta G_{i,(T)}^{\text{fusion}} = \left(\Delta H_{i,(T_m)}^{\text{fusion}} + \int_{T_m}^T \Delta C_{p,i} dT \right) - T \left(\frac{\Delta H_{i,(T_m)}^{\text{fusion}}}{T_m} + \int_{T_m}^T \frac{\Delta C_{p,i} dT}{T} \right) \tag{19}$$

where $\Delta C_{p,i}$ is the difference of heat capacity between the liquid and the crystalline forms of component i .

Through an extensive review of the literature, we have selected the most recently and accurately acquired thermodynamic properties of $\text{CaAl}_2\text{Si}_2\text{O}_8$ (anorthite) and

NaAlSi₃O₈ (albite) components (e.g., Boettcher et al. 1982; Stebbins et al. 1982; Richet and Bottinga 1984a, b; Berman 1988; Lange 2003; Tenner et al. 2007; Table 2). These data have been used to calculate the variations of $\Delta G_{\text{Ab},(T)}^{\text{fusion}}$ and $\Delta G_{\text{An},(T)}^{\text{fusion}}$ as a function of temperature (Fig. 3). These parameters decrease continuously and significantly from 1,000 to 1,600 K, a temperature interval considered as relevant to most magmatic processes. In contrast, the value of $(\Delta G_{\text{An},(T)}^{\text{fusion}} - \Delta G_{\text{Ab},(T)}^{\text{fusion}})$ is approximately constant (between 26 and 30 kJ/mol) in the considered temperature interval.

Activity-composition relation in plagioclase

The plagioclase solid solution is not ideal and is characterized by a structural transition between $C\bar{1}$ for albitic compositions and $I\bar{1}$ for anorthitic compositions (Orville 1972). The composition of plagioclase at which this transition occurs is a linear function of temperature (Carpenter and McConnell 1984). The most significant difference between the two structural states is that plagioclase from the $C\bar{1}$ region is characterized by a disordered distribution of Si and Al tetrahedra, while plagioclase from the $I\bar{1}$ region shows relatively high degrees of order (Carpenter 1988). Both structural state and degree of ordering have an influence on the activities of albite and anorthite components, and various models have been proposed to calculate activities as a function of plagioclase composition and temperature. For example, using Darken's quadratic formalism described by Powell (1987), Holland and Powell (1992) have divided the plagioclase solid solution into two different regions ($C\bar{1}$ and $I\bar{1}$) in which regular behavior was assumed (Powell 1987). In this way, Holland and Powell (1992) proposed fully consistent equations allowing to

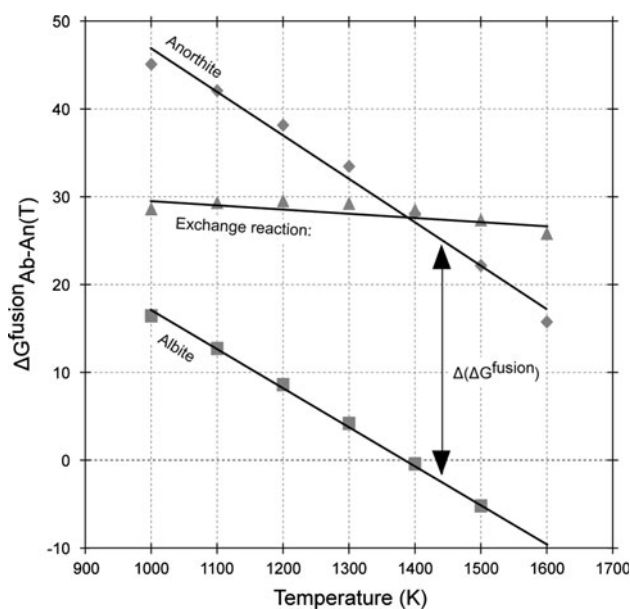


Fig. 3 Calculated Gibbs free energies of melting of albite and anorthite components as a function of temperature. The difference between Gibbs free energies of melting of anorthite and albite is also represented. See Table 2 for description of the thermodynamic data used in calculations

calculate activities of albite and anorthite components across the entire plagioclase solid solution and for temperatures from 1,173 to 1,573 K (Fig. 4). It is important to note that the difference between activity and concentration decreases with increasing temperature, this difference being relatively low for the temperature range of interest to most magmatic applications. The activity-composition relations of Holland and Powell (1992) are extremely valuable, but they are difficult to implement in the construction of a predictive model for plagioclase composition for the two following reasons: (1) the structural state of

Table 2 Selected thermodynamic properties for albite and anorthite

Parameter	Value or equation	Unit	Reference
Albite			
Melting temperature	1373	K	Boettcher et al. (1982)
Enthalpy of fusion	64.5	kJ/mol	Tenner et al. (2007)
Entropy of fusion	47.0	J/(mol K)	Calculated
Heat capacity of the solid phase	$393.64 - 2451T^{-0.5} - 7.8928 \cdot 10^6 T^{-2} + 1.07064 \cdot 10^9 T^{-3}$	J/(mol K)	Bermann (1988)
Heat capacity of the liquid phase	359	J/(mol K)	Tenner et al. (2007)
Anorthite			
Melting temperature	1830	K	Richet and Bottinga (1984b)
Enthalpy of fusion	133	kJ/mol	Richet and Bottinga (1984b)
Entropy of fusion	72.67	J/(mol K)	Calculated
Heat capacity of the solid phase	$439.37 - 3734.1T^{-0.5} + 3.1702 \cdot 10^8 T^{-3}$	J/(mol K)	Bermann (1988)
Heat capacity of the liquid phase	432	J/(mol K)	Richet and Bottinga (1984b)

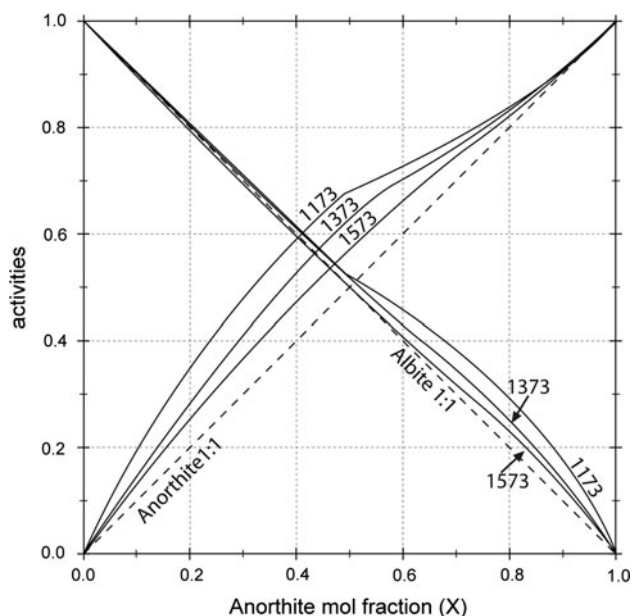


Fig. 4 Predicted evolution of anorthite and albite activities in plagioclase as a function of plagioclase composition (anorthite mol fraction; X) and temperature (in K). Curves were calculated following the equations of the Darken’s quadratic formalism described by Holland and Powell (1992) and considering a disordered mixing of Si and Al on tetrahedral sites in the plagioclase $\bar{C}I$ region and an ordered mixing of Si and Al on tetrahedral sites in the $\bar{I}I$ region

plagioclase must be known to use the relevant activity-composition relation, i.e., a first estimation of plagioclase composition must be available; (2) for plagioclase of the $\bar{I}I$ structure, a_{Ab} and a_{An} are related to the plagioclase composition (X) by fifth-order equations that may not be simply solved.

In this paper, we have used simplified equations linking activity and composition by considering that plagioclase solid solution represents an ideal mixture on one-cation site per 8-oxygen formula unit. In this case, it may be shown that (Kerrick and Darken 1975; Price 1985):

$$a_{An}^{Pl} = X_{An} \tag{20a}$$

$$a_{Ab}^{Pl} = X_{Ab} \tag{20b}$$

where X_{An} and X_{Ab} are the plagioclase composition (An mol = [molar Ca/(Ca + Na + K)]; Ab mol = [molar Na/(Ca + Na + K)]).

Figure 5 shows the values of a_{Ab} and a_{An} for plagioclases of the experimental database calculated using simplified equations (Eqs. 20a, 20b) compared to those obtained with the more complete equations of Holland and Powell (1992). Values of a_{Ab} are practically identical for the two methods of calculation. Values of a_{An} are practically identical at high a_{An} , and the difference increases when a_{An} decreases, but never exceeds 10%.

Activities of albite and anorthite in the liquid

The thermodynamics of silicate melts has been frequently considered in terms of complex components that reflect mineral stoichiometries (i.e., the “quasi-crystalline” model; e.g., Hess 1977; Burnham 1981; Mysen 1990; Ghiorsso and Sack 1995). Application of this approach requires knowledge of how the activities of the components $CaAl_2Si_2O_8$ (anorthite) and $NaAlSi_3O_8$ (albite) vary in the liquid as a function of melt composition. However, little direct information is available relevant to this question, and no working theory is currently available to predict the activities of melt components across a large range of liquid composition (e.g., basalt to rhyolite). Alternatively, the activities of complex components can be expressed in terms of the activities of simpler oxide components. Considering the stoichiometry of “anorthite” and “albite” in the melt, it may be shown that:

$$\ln a_{An}^{Liq} = \ln a_{CaO}^{Liq} + \ln(a_{AlO_{1.5}}^{Liq})^2 + \ln(a_{SiO_2}^{Liq})^2 \tag{21a}$$

$$\ln a_{Ab}^{Liq} = \ln a_{NaO_{0.5}}^{Liq} + \ln a_{AlO_{1.5}}^{Liq} + \ln(a_{SiO_2}^{Liq})^3 \tag{21b}$$

leading to:

$$\ln \left(\frac{a_{An}^{Liq}}{a_{Ab}^{Liq}} \right) = \ln a_{CaO}^{Liq} + \ln a_{AlO_{1.5}}^{Liq} - \ln a_{NaO_{0.5}}^{Liq} - \ln a_{SiO_2}^{Liq} \tag{22}$$

Equation 22 suggests that the variation of $\ln \left(\frac{a_{An}^{Liq}}{a_{Ab}^{Liq}} \right)$ is directly related to the natural logarithms of activities of CaO , $AlO_{1.5}$, SiO_2 , and $NaO_{0.5}$ melt components. As a first attempt, we have applied Eq. 22 to all the experimental liquids of the database by using mole fractions of metal-oxide components and an additional constant term on the right-hand side to take account of activity coefficients:

$$\ln \left(\frac{a_{An}^{Liq}}{a_{Ab}^{Liq}} \right) = \ln X_{CaO}^{Liq} + \ln X_{AlO_{1.5}}^{Liq} - \ln X_{NaO_{0.5}}^{Liq} - \ln X_{SiO_2}^{Liq} + d \tag{23}$$

where d is a constant calculated for each plagioclase-liquid pair, representing:

$$d = \ln \gamma_{CaO}^{Liq} + \ln \gamma_{AlO_{1.5}}^{Liq} - \ln \gamma_{NaO_{0.5}}^{Liq} - \ln \gamma_{SiO_2}^{Liq} \tag{24}$$

The results of this investigation show that the calculated values for the d parameter of Eq. 23 vary from -2.29 to 0.69 . Application of Eq. 23 thus indicates that $\sum_1^i \ln \gamma_i^{Liq}$ (with i being CaO , $AlO_{1.5}$, $NaO_{0.5}$, and SiO_2) is not a constant and that the activities of plagioclase components in the liquid phase cannot be considered as being simply related to the molar fractions of CaO , $AlO_{1.5}$, $NaO_{0.5}$, and SiO_2 in the melt. This is of no surprise as the structure of silicate melts is known to be relatively complex with

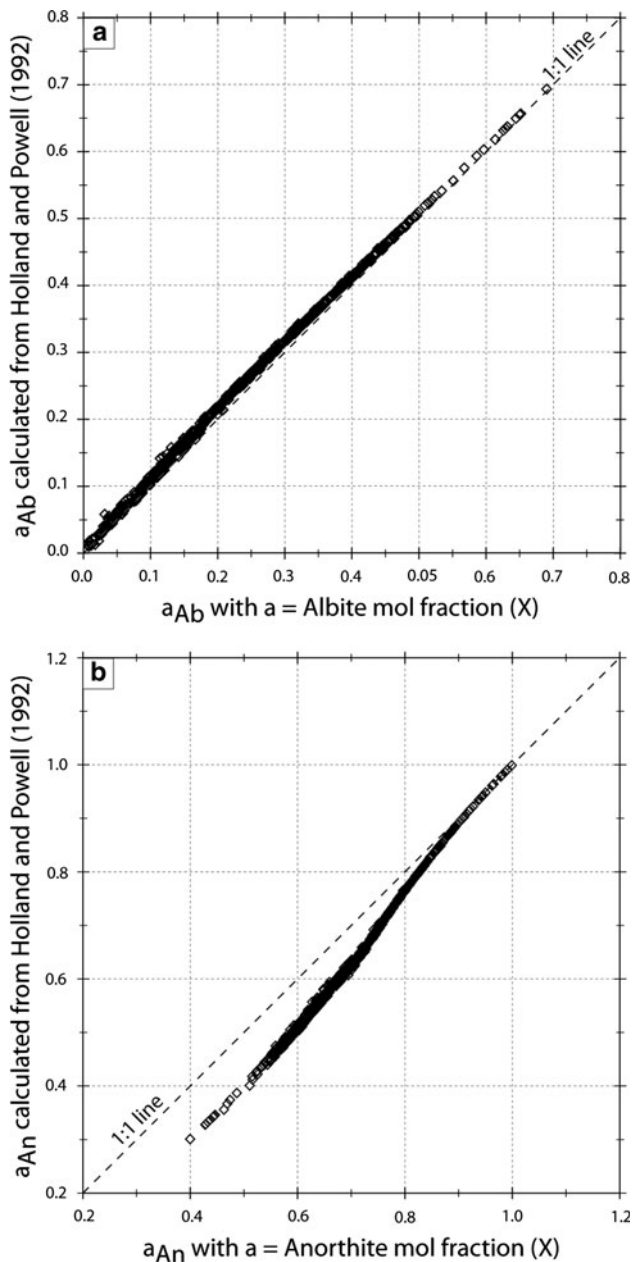


Fig. 5 **a** Binary diagram showing the evolution of activity of albite in experimental plagioclases ($n = 530$) calculated using the assumption that activity = albite mol fraction vs. activity of albite in experimental plagioclases calculated using equations of Holland and Powell (1992) taking into account that the solid solution between albite and anorthite is not ideal. **b** Same diagram showing the evolution of the activity of anorthite in experimental plagioclases

different cations playing different and sometimes multiple structural roles (e.g., Mysen and Richet 2005). Interactions between cations translate into activity coefficients for individual oxides that are complex functions of overall melt chemistry, explaining the failure of the d term of Eq. 23 to be constant.

An alternative approach is therefore to consider thermodynamic activities of relevant individual oxides (i.e., Eq. 22). The literature provides some indications of how activities of a variety of metal cations may vary in silicate melts (e.g., Holzheid et al. 1997; Courtial et al. 1999; Holzheid and Grove 2005). For the elements of interest here, and given the silica and alumina-rich nature of geological liquid relative to metallurgical slags, we have chosen to focus on the studies of Libourel (1999), Toplis (2005), and Mathieu (2009), which provide constraints on the activities of Ca, Si, and Na, respectively. However, it should be noted that these equations do not give a direct expression of the activities of the different oxide components, but rather an indirect measure that could be called a pseudo-activity (a^*). Moreover, these models were generally calibrated using restricted ranges of melt composition. Extrapolation to the large range of liquid compositions compiled for this study is therefore not straightforward. To take account of the fact that these models may give values proportional but not identical to activities, we have chosen to regress data to Eq. 25 (rather than Eq. 22):

$$\ln \left(\frac{a_{\text{An}}^{\text{Liq}}}{a_{\text{Ab}}^{\text{Liq}}} \right) = b \left[\ln a_{\text{CaO}}^{*\text{Liq}} \right] + c \left[\ln a_{\text{NaO}_{0.5}}^{*\text{Liq}} \right] + d \left[\ln a_{\text{AlO}_{1.5}}^{*\text{Liq}} \right] + e \left[\ln a_{\text{SiO}_2}^{*\text{Liq}} \right] + f \quad (25)$$

where b , c , d , e , and f are fit parameters calculated by least-squares regression analysis. Regressions of Eq. 25 were performed for different groups of melt compositions, and contrasted results were obtained: (1) when all the experimental melts are considered simultaneously, $r^2 = 0.74$; (2) when mafic–ultramafic melts are considered separately, $r^2 = 0.88$ (see above for the description of the melt compositional groups); (3) high alkali mafic–ultramafic melts ($r^2 = 0.81$); (4) intermediate to felsic melts ($r^2 = 0.51$). Poor regression coefficients (r^2) were thus obtained for each case, indicating that the currently available models for oxide pseudo-activities are insufficient to provide satisfactory prediction of values for $\ln \left(\frac{a_{\text{An}}^{\text{Liq}}}{a_{\text{Ab}}^{\text{Liq}}} \right)$, and that further work is required to constrain the relevant activity coefficients of $\text{AlO}_{1.5}$, SiO_2 , $\text{NaO}_{0.5}$, and CaO in natural silicate melts.

Empirical fits to oxide activity terms

In light of the failure to produce a model based upon known variations of oxide activities, it is of interest to assess whether the liquid-related terms of Eq. 14 (for $a_{\text{An}}^{\text{Liq}}$ and $a_{\text{Ab}}^{\text{Liq}}$ individually) and Eq. 16 can be fitted empirically as a function of melt composition (e.g., Putirka 1999; Putirka et al. 2003). For example, for the case of Eq. 16,

the possibility of finding a simple empirical expression to calculate the $(\ln a_{\text{CaO}}^{\text{Liq}} + \ln a_{\text{AlO}_{1.5}}^{\text{Liq}} - \ln a_{\text{NaO}_{0.5}}^{\text{Liq}} - \ln a_{\text{SiO}_2}^{\text{Liq}})$ term of Eq. 22 has been explored. We have defined (e.g., Housh and Luhr 1991; Ghiorso et al. 1983; Holzheid et al. 1997; Lange et al. 2009):

$$\ln \left(\frac{a_{\text{An}}^{\text{Liq}}}{a_{\text{Ab}}^{\text{Liq}}} \right) = a + \frac{b}{T} + \sum c_i Y_i \quad (26)$$

$$\ln a_j^{\text{Liq}} = a + \frac{b}{T} + \sum c_i Y_i \quad (27)$$

where a , b , and c are fit parameters from least-squares regression, Y_i are liquid components. In Eq. 27, j represents albite or anorthite components.

A two-stage treatment has been applied to the liquid components (e.g., SiO_2 , Al_2O_3 , etc.) before implementing them into Eqs. 26 and 27 (see example in Table A3; Suppl. Mat.): (1) Liquid components in wt% (e.g., SiO_2 , Al_2O_3 , etc.) were converted into mole fractions of each oxide component. Oxide weight percentages were not renormalized to 100 wt% prior to calculations of mole fractions. Iron was treated as FeO_t (e.g., Glazner 1984; Lange et al. 2009); (2) the mole fractions of oxide components were normalized to cation proportions (e.g., Si, Al, etc.) on an 8-oxygen basis. The cation proportions obtained after stage 2 were integrated into Eqs. 26 and 27 for regression. The family of Y_i terms in Eqs. 26 and 27 also contains two ratios of melt components involved in the albite-anorthite solid solution ($[\text{Ca}/(\text{Ca} + \text{Na})]$ and $[\text{Al}/(\text{Al} + \text{Si})]$), a choice justified by the fact that including these ratios significantly improves the quality of the regressions, as previously observed by Putirka (2005).

Fitting Eq. 26 to the entire liquid data set gives poor results ($r^2 = 0.85$), which indicates that the calculated regression coefficients cannot be used as a basis for building a predictive model for plagioclase composition. In light of this fact, regressions of Eq. 27 have been separately performed for $a_{\text{An}}^{\text{Liq}}$ and $a_{\text{Ab}}^{\text{Liq}}$. Results for the albite component gave mediocre results ($r^2 = 0.70$). On the contrary, very good results were obtained for regressions of anorthite activities ($r^2 = 0.99$; Table A4; Suppl. Mat.). The low quality of regression for the albite component could result from at least 4 reasons: (1) the Na-content is relatively low in most experimental plagioclases and in some experimental liquids, so the precision of analyses of Na is lower than that of Ca; (2) Na volatilizes during furnace runs; (3) Na diffuses away from the electron beam during microprobe analysis; and (4) the concentration of Na in the crystals is inversely correlated with temperature, so the activities in the crystals are highest at the lowest temperatures, where equilibrium is most difficult to attain.

The excellent quality of regression of Eq. 27 for the anorthite component provides the basis for a robust predictive model for plagioclase composition. Before establishing the complete mathematical expression of such a model, a statistical refinement of the fitted coefficients of Eq. 27 has been performed in order to identify the relative contribution of each melt component to the values of anorthite activity in silicate melts. The statistic significance of each of the terms of Eq. 27 was assessed with the t -test (ratio of fitted term over its standard error, with 1.2 chosen as the cut-off value). Furthermore, the independent contribution of each parameter was assessed through consideration of partial correlations between dependent and independent parameters.

A second multiple linear regression of Eq. 27 was then performed by including only parameters having successfully passed through both the t -student and the partial correlation-test. For this calibration, only 70% of the experiments (selected randomly) were used. The remaining 30% were used later as an independent “test dataset.” Using the results of this regression, it was found that uncertainties on the test dataset (Table A4; Suppl. Mat.) are very similar to those obtained during calibration. For this reason, a final calibration was performed using the complete experimental database, leading to slight improvement of the quality of prediction of anorthite activities (Fig. 6; Table A4; Suppl. Mat.). The expression derived to calculate anorthite activities in low-pressure natural silicate melts is:

$$\begin{aligned} \ln a_{\text{An}}^{\text{Liq}} = & 5.72 - \frac{15339}{T} + \left[0.41\text{Si}_8 - 1.69\text{Al}_8 \right. \\ & - 0.34\text{Fe}_8 - 0.51\text{Mg}_8 - 0.50\text{Ca}_8 + 0.54\text{Na}_8 \\ & \left. + 1.99 \frac{\text{Ca}_8}{\text{Ca}_8 + \text{Na}_8} + 8.20 \frac{\text{Al}_8}{\text{Al}_8 + \text{Si}_8} \right] \quad (28) \end{aligned}$$

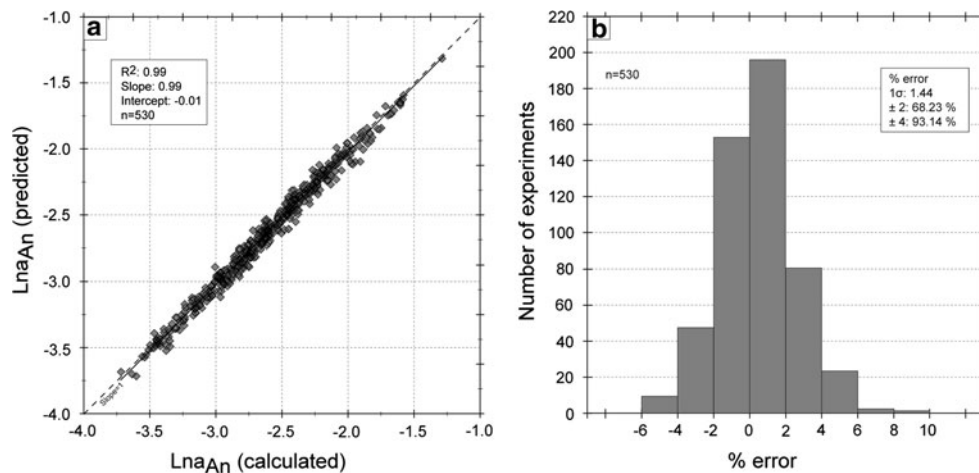
where the subscript 8 indicates that melt components are cation fractions normalized on an 8-oxygen basis.

Internal test of the activity regression

The internal consistency of Eq. 28 may be tested by calculating theoretical values for the enthalpy and entropy of fusion of anorthite and by comparing these values with calorimetric data. Using the coefficient of the inverse T term, a value of 128 kJ/mol is calculated for the enthalpy of fusion of anorthite. This value is close to the value of 133 kJ/mol derived by calorimetry (Richet and Bottinga 1984b). The entropy of fusion of anorthite has been calculated by considering the theoretical cation fractions of Ca, Al, and Si in a liquid having a composition of pure anorthite ($\text{Ca}_8 = 1$, $\text{Al}_8 = 2$; $\text{Si}_8 = 2$). Following this reasoning, a value of 72.7 J/(mol.K) is obtained. This value

Fig. 6 Results of the predictive model for the calculation of the activity of anorthite in experimental melts

a Correlation between melt anorthite activities calculated using Eqs. 14 and subsequent and melt anorthite activities predicted using Eq. 28.
b Histogram showing the total range of error (%) predicted by the model for calculation of the melt anorthite activities. See Table A4 (Suppl. Mat.) for a detailed statistical description of the errors



is inside the range of values proposed in the literature and is moreover very close to the most commonly accepted value of 73 J/(mol.K) determined by Richet and Bottinga (1984b). The good correspondence between the calculated values for the enthalpy and the entropy of fusion of anorthite with those determined from calorimetric data suggests that the regression parameters of Eq. 28 are thermodynamically reasonable and may thus be used as part of a robust predictive model for plagioclase composition.

Construction of a predictive model for plagioclase composition

As discussed above, the plagioclase compositions in equilibrium with silicate melts can be calculated using a slightly rearranged version of Eq. 14:

$$\ln X_{An} = \ln a_{An}^{Sol} = \frac{\Delta G_{An,(T)}^{fusion}}{RT} + \ln a_{An}^{Liq} \quad (29)$$

Mathematical expressions for $\Delta G_{An,(T)}^{fusion}/RT$ and $\ln a_{An}^{Liq}$ are required to solve Eq. 29. The complete expression for $\Delta G_{An,(T)}^{fusion}$ is shown in Fig. 3, and details of the calculation procedure are given in Eq. 19. In order to facilitate the applicability of Eq. 29, the $\Delta G_{An,(T)}^{fusion}/RT$ term on the left-hand side has been fitted to a simple function of temperature ($r^2 = 0.99$) by least-squares regression analysis (e.g., Holzheid et al. 1997):

$$\frac{\Delta G_{An,(T)}^{fusion}}{RT} = 46.58 - 0.0018T - 5.77 \ln T \quad (30)$$

Concerning the expression of $\ln a_{An}^{Liq}$, a function involving temperature and liquid components (Eq. 28) was fitted to all calculated values of the experimental melts of the database (Fig. 6).

By combining the regression coefficients of Eqs. 28 and 30 into Eq. 29, the complete mathematical expression that

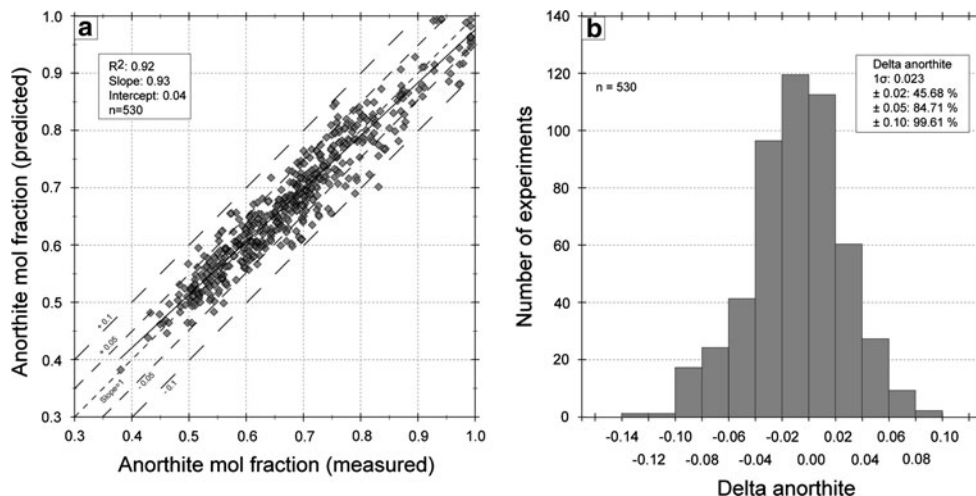
allows calculating plagioclase compositions in equilibrium with silicate melts can be expressed as follows:

$$\begin{aligned} \ln X_{An} = & [46.58 - 0.0018T - 5.77 \ln T] \\ & + [5.72 - 15339T^{-1}] + \left[0.41Si_8 - 1.69Al_8 \right. \\ & - 0.34Fe_8 - 0.51Mg_8 - 0.50Ca_8 + 0.54Na_8 \\ & \left. + 1.99 \frac{Ca_8}{Ca_8 + Na_8} + 8.20 \frac{Al_8}{Al_8 + Si_8} \right] \quad (31) \end{aligned}$$

where T is the temperature in Kelvin and Si_8 , Al_8 , etc. are cationic melt components normalized on an 8-oxygen basis. An Excel spreadsheet allowing calculation of plagioclase compositions can be found in Electronic Annex.

The agreement between calculated and measured values of plagioclase composition is illustrated in Fig. 7. Detailed analysis shows that 46% of the values are reproduced within $\pm 2\%$ of the measured ones, 86% to within $\pm 5\%$, and 99% to within $\pm 10\%$. The ability of Eq. 31 to predict the composition of plagioclases that crystallize in equilibrium with silicate melts is significantly higher than that of previous models (Table 1; Fig. A4; Suppl. Mat.). At least 5 reasons have been identified to account for these good results: (1) Eq. 31 was calibrated with a database that only contains anhydrous experiments equilibrated at 1-atm, which has the effect to reduce the number of parameters influencing the composition of equilibrium plagioclase; (2) the calibration database contains a large number of plagioclase-liquid pairs ($n = 530$), and both the liquid and the solid phases cover a large range of compositions, consequently avoiding significant extrapolation outside the calibration range; (3) different filters have been applied to the calibration database to ensure that plagioclase and liquid are in an equilibrium state; (4) liquid components were normalized on an 8-oxygen basis, which allows a more straightforward identification of the melt components that have a statistical influence on anorthite activities in the liquid phase; (5) only the most recently and accurately

Fig. 7 Results of the thermodynamically derived model for the prediction of plagioclase composition as a function of melt composition and temperature (Eq. 31). **a** Correlation between observed compositions of experimental plagioclases and those predicted using Eq. 31. **b** Histogram showing the total range of error (delta anorthite; $An_{mol. predicted} - An_{mol. observed}$) predicted by the model



acquired standard-state thermodynamic data for anorthite have been selected.

T-independent empirical models

Regression strategies

In addition to the knowledge of the liquid composition, the thermodynamically derived model outlined above (Eq. 31) requires precise estimation of the equilibrium temperature between plagioclase and liquid. This parameter is frequently unknown or poorly constrained in many petrological applications; thus, we also describe a simplified temperature-independent model that is only based on least-squares regression of melt components. The general form of the equation is:

$$X_{An} = a + \sum b_i Y_i \tag{32}$$

where *a* and *b* are regression coefficients and *Y_i* are cationic melt components. A similar normalization procedure (8-oxygen basis) to that outlined above has been applied to the melt components.

As a first attempt, we have tried to regress a single equation to calculate the plagioclase compositions in equilibrium with all silicate melts of the database (SiO₂: 43–78 wt%), but very poor results were obtained. This is of no surprise as temperature exerts a primary control on plagioclase composition (see Eq. 31), and basaltic melts crystallize plagioclase at a temperature of ca. 1,150–1,200°C (e.g., Toplis and Carroll 1995) while rhyolitic melts crystallize plagioclase at significantly lower temperatures (typically 950–1,000°C; e.g., Brugger et al. 2003). We therefore consider more restricted melt compositional groups, where narrower temperature ranges for plagioclase saturation are expected. As discussed above, the experimental database has thus been subdivided into three groups: (1) alkali-poor mafic–

ultramafic melts; (2) alkali-rich mafic–ultramafic melts; and (3) intermediate to felsic melts (Fig. 1).

For each melt compositional group, an initial regression of Eq. 32 has been performed using 70% of the experiments (calibration dataset; selected randomly). Values of fitted parameters are given in Table A5 (Suppl. Mat.). The models were subsequently tested with the 30% of the plagioclase-liquid pairs left after the random selection (test dataset). In each melt compositional group, errors obtained with the test dataset are extremely similar to those obtained with the calibration dataset. A final regression of Eq. 32 was thus performed with all the experimental plagioclase-liquid pairs of each liquid compositional group. Fitted parameters are given in Eqs. 33–35 (below), and a detailed statistical description of these parameters is presented in Table A5 (Suppl. Mat.).

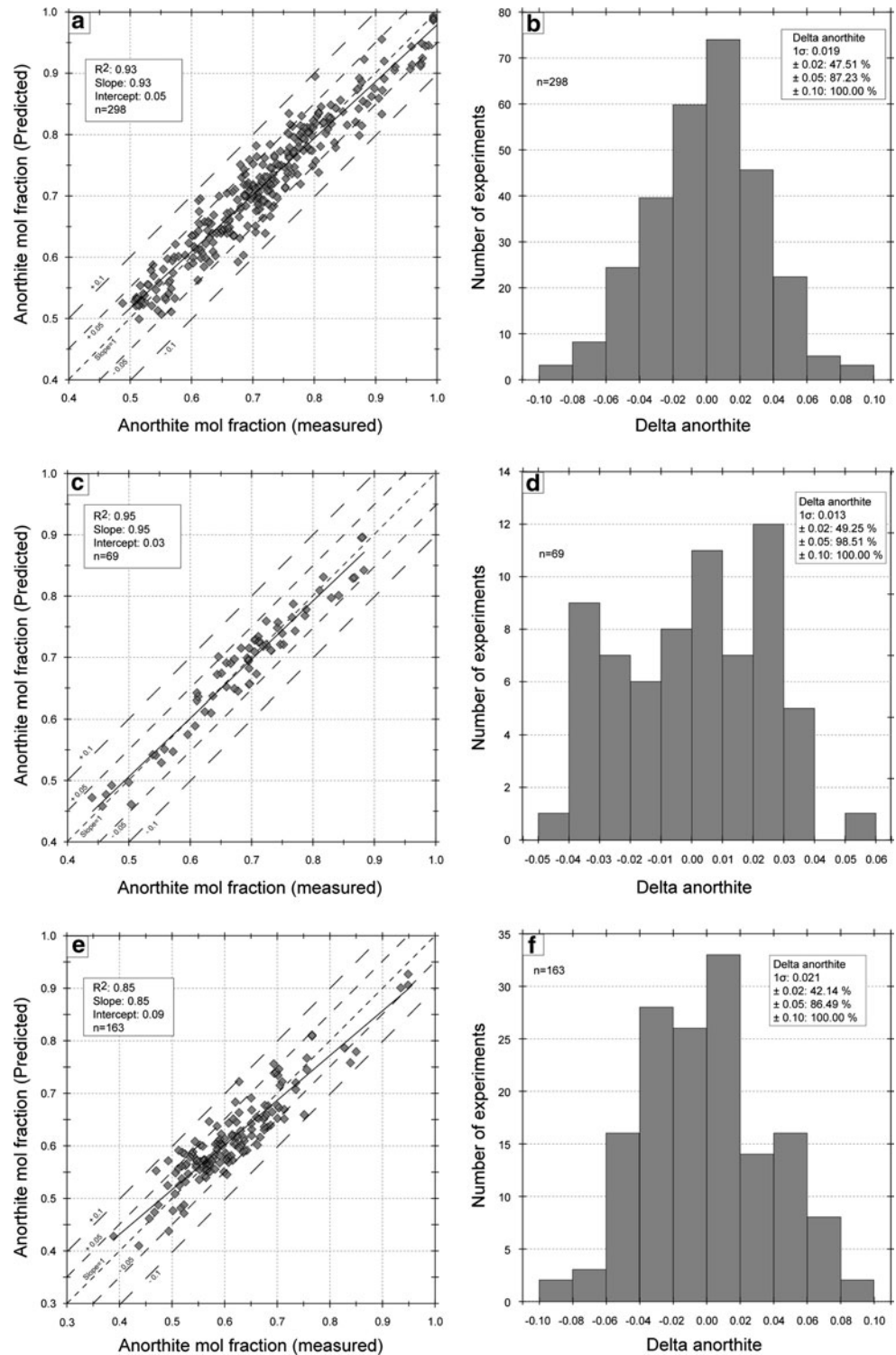
Regression models

For the group of mafic–ultramafic melts, we used 298 experimental plagioclase-liquid pairs to calibrate the following expression:

$$X_{An} = -2.71 + \left[0.55Si_8 - 0.04Al_8 + 0.35Fe_8 + 0.19Mg_8 + 0.19Ca_8 + 0.45Na_8 \right] + \left[1.09 \frac{Ca_8}{Ca_8 + Na_8} + 3.68 \frac{Al_8}{Al_8 + Si_8} \right] \tag{33}$$

A good correlation (*r*² = 0.93) was obtained between predicted An-contents of plagioclase (Eq. 33) and those experimentally observed (Fig. 8a). The linear regression has a slope of 0.93 and an intercept of 0.05. The total range of error in prediction of plagioclase composition is relatively low (–0.08 to 0.09; Fig. 8b) when compared with previous plagioclase-melt equilibria models (Table 1; Fig. A4; Suppl. Mat.). It is moreover interesting to note that ~50% of the plagioclase compositions are predicted within an error of ± 2% and ~90% within ± 5%.

Fig. 8 Results of T-independent empirical models plagioclase-melt equilibria. **a** Mafic and ultramafic melts. Correlation between observed compositions of experimental plagioclases and those predicted by Eq. 33. **b** Histogram showing the total range of error predicted by the model. **c–d** alkali-rich mafic and ultramafic melts (Eq. 34). **e–f** Intermediate to felsic melts (Eq. 35). See Table A5 (Suppl. Mat.) for a detailed statistical description of the errors



For the group of alkali-rich mafic–ultramafic magmas, the model was calibrated on the basis of a lower number of experiments ($n = 69$), owing to scarcity of 1-atm anhydrous experiments with this kind of composition in the literature. The equation for predicting plagioclase compositions is the following:

$$\begin{aligned}
 X_{An} = & -4.66 + [1.16Si_8 - 3.14Al_8 - 0.34Fe_8 - 0.16Mg_8 \\
 & - 0.82Ca_8 + 0.58Na_8] \\
 & + \left[2.17 \frac{Ca_8}{Ca_8 + Na_8} + 16.48 \frac{Al_8}{Al_8 + Si_8} \right] \quad (34)
 \end{aligned}$$

A very good correlation was obtained between predicted plagioclase An-contents (Eq. 34) and those experimentally observed ($r^2 = 0.95$; Fig. 8c). The linear regression is very close to the theoretical 1:1 line (slope: 0.95; intercept: 0.03), and this calibration gives accurate results for a large range of plagioclase compositions (0.44–0.89 An mol). The total range of error is narrow (−0.05 to 0.06; Fig. 8d). It is of note that 50% of the plagioclase compositions are predicted within an inaccuracy of $\pm 2\%$ and $\sim 100\%$ within $\pm 5\%$.

For the group of intermediate to felsic magmas, the empirical model was calibrated on the basis of 163 plagioclase-melt assemblages. Plagioclase compositions may be calculated using the following expression:

$$X_{An} = 1.17 + [-0.22Si_8 + 0.94Al_8 - 0.49Fe_8 + 0.07Mg_8 + 0.41Ca_8 - 0.04Na_8] + \left[0.31 \frac{Ca_8}{Ca_8 + Na_8} - 3.86 \frac{Al_8}{Al_8 + Si_8} \right] \quad (35)$$

The accuracy of Eq. 35 is slightly lower than that obtained for Eqs. 33–34. This is related to the calibration database that contains a larger range of liquid compositions, which suggests that the suppression of the T-parameter has probably a more significant effect than for the two other melt compositional groups. Figure 8e shows the correlation ($r^2 = 0.85$) between experimental plagioclase compositions and those predicted by the model. The linear regression has parameters (slope: 0.85; intercept: 0.09) that are relatively far from the theoretical 1:1 line. It can, however, be noted that out of the 169 experiments considered in this model, all the plagioclase compositions are predicted within $\pm 10\%$ and that more than 85% to within $\pm 5\%$ (Fig. 8f). We moreover note that none of the previously published models allows more accurate predictions for the compositions of plagioclase in equilibrium with the intermediate to felsic experimental liquids.

Test of the empirical models across critical boundaries

Magmatic differentiation is responsible for a geochemical evolution of residual liquids toward more evolved compositions. In some cases, this evolution is responsible for an increase of the melt SiO_2 - and $(Na_2O + K_2O)$ -contents (see the example of Thingmuli, Iceland, Carmichael 1964; Fig. 9), and residual liquids may cross our arbitrarily chosen boundaries between empirical models (52 wt% SiO_2 ; 5 wt% $Na_2O + K_2O$). Because these models are aimed at predicting the compositions of plagioclase crystallizing along whole liquid lines of descent, it is of interest to verify whether equations provide comparable results in the vicinity of their boundaries (i.e., Eqs. 33–34; Eqs. 33–35; Eqs. 34–35). This has been tested for liquid compositions in the range: SiO_2 : 50–54 wt%; $Na_2O + K_2O$: 4–6 wt%

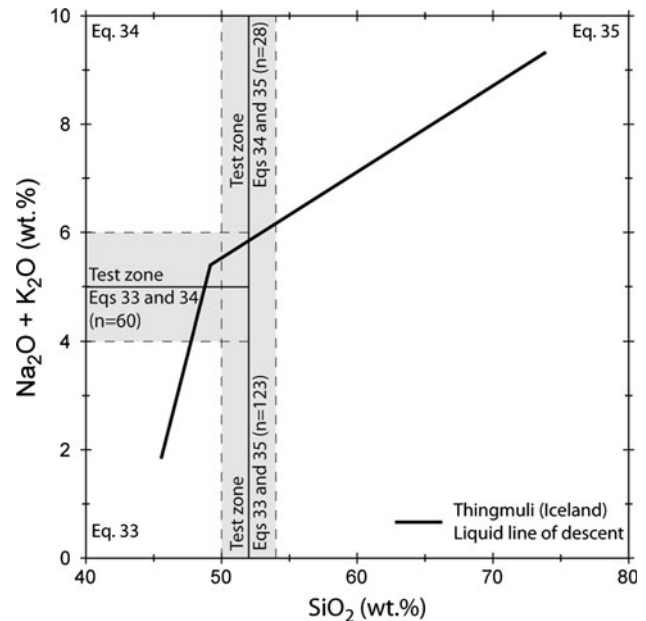


Fig. 9 $Na_2O + K_2O$ vs SiO_2 binary diagram showing an example of liquid line of descent (Thingmuli Volcano, Iceland, after the data of Carmichael 1964) crossing the critical boundaries between the empirical T-independent predictive models for plagioclase compositions (Eqs. 33–35). The compositional ranges of liquids used to test equations from both sides of the critical boundaries (52 wt% SiO_2 and 5 wt% $Na_2O + K_2O$) are also shown

(Fig. 9). Results of this investigation are shown in Table 3. In all cases, differences in predicted An-contents when using two different equations are small (average: 0.03; 1σ : 0.02) demonstrating that the T-independent empirical equations proposed here (Eqs. 33–35) may indeed be used to model liquid lines of descent characterized by significant ranges of SiO_2 - and $(Na_2O + K_2O)$.

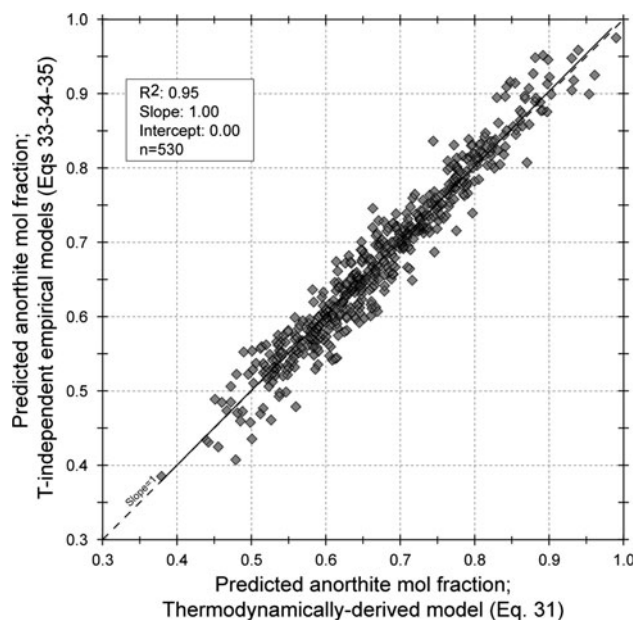
Conclusions

Expressions for plagioclase-liquid equilibrium are developed from least-squares regression analysis of experimental plagioclase + liquid pairs equilibrated at 1-atm in anhydrous natural and synthetic systems. Four new equations have been derived and allow the compositions of plagioclase crystallizing in equilibrium with silicate melts to be calculated. The calibration database covers a large range of melt compositions (from basalt to rhyolite) and a large range of temperature (998–1,355°C); thus, the models are applicable to the modeling of liquids differentiating within the upper crust, with little or no extrapolation.

The novel aspect of this contribution is the characterization of the role of melt composition on the composition of plagioclase feldspars. The first equation is thermodynamically derived and takes into account the influence of

Table 3 Comparison of predicted plagioclase compositions by Eqs. 33–35 at critical boundaries (52 wt% SiO₂ and 5 wt% Na₂O + K₂O)

Models across the critical boundary	Liquid compositions		Differences in predicted plagioclase An-contents									
	SiO ₂ (wt%)	Na ₂ O + K ₂ O (wt%)	Linear regression		Maximum ^d		Within ± 2% ^f		Within ± 5% ^g			
			n	Slope	Intercept	Average ^a	1σ ^b	Minimum ^c	Maximum ^d	Within ± 1% ^e	Within ± 2% ^f	Within ± 5% ^g
Mafic-ultramafic (Eq. 32)	<52	4–6	60	1.21	-0.12	0.03	0.02	0.00	0.08	21	35	82
Mafic-ultramafic (Eq. 32)	50–54	<5	123	0.94	0.01	0.03	0.02	0.00	0.09	10	33	73
Alkali-rich mafic-ultramafic (Eq. 33)	50–54	>5	28	0.91	0.05	0.03	0.02	0.00	0.08	18	39	89

^a Average difference between the two models^b 1σ standard deviation of the differences taken in absolute value^{c,d} Minimum and maximum differences taken in absolute values^{e,f,g} Percentage of the data with differences in the intervals of -1 and +1%, -2 and +2%, and -5 and +5%**Fig. 10** Comparison between the plagioclase compositions predicted by the thermodynamically derived model (Eq. 31) and the empirical T-independent models (Eqs. 33–35)

temperature, in addition to that of liquid composition. The experimental database is used to derive a model that allows calculation of the activity of anorthite in the liquid phase. Although discussion of the links between the melt structure and the new model for anorthite activities in the liquid phase is outside the scope of the current manuscript, it is of interest to note that the activity of anorthite depends on many melt components and not only to the concentration of CaO, Na₂O, SiO₂, and Al₂O₃. Combination of standard-state thermodynamic properties together with activity models for both the solid and the liquid phases was used to derive a mathematical equation that can be used to calculate plagioclase compositions with a relative inaccuracy generally lower than 10% ($1\sigma = 0.023$).

While accurate, the thermodynamically derived equation requires a precise estimate of the temperature of plagioclase-melt equilibrium. This parameter is frequently unknown or inaccurately estimated in many petrological studies. Empirical equations were thus calibrated allowing prediction of plagioclase composition as a function of melt composition, independently of any temperature estimation. Due to the critical effect of temperature on plagioclase-melt equilibria, empirical regressions were performed for three subgroups of experimental liquid compositions (mafic, alkali-rich mafic, and felsic) where less temperature variation is expected. The accuracy of empirical models ($1\sigma = 0.019$; 0.013; 0.021) is similar to that of the thermodynamically derived model. Empirical and thermodynamic models thus give relatively similar plagioclase compositions for all the liquids of the experimental database (Fig. 10).

Acknowledgments This work was financed by the *Belgian Fund for Joint Research (FNRS)* and the *Fund for Research in Industry and Agriculture (FRIA)*. H.S. O'Neill is acknowledged for stimulating discussions during the stay of ON at RSES (Australian National University). Very detailed reviews by K. Putirka and an anonymous reviewer significantly improved the quality of the manuscript. Comments and editorial handling by T. Grove were also highly appreciated.

References

- Bédard JH (2006) Trace element partitioning in plagioclase and feldspar. *Geochim Cosmochim Acta* 70:3717–3742
- Berman RG (1988) Internally consistent thermodynamic data for minerals in the system $\text{Na}_2\text{O}-\text{K}_2\text{O}-\text{CaO}-\text{MgO}-\text{FeO}-\text{Fe}_2\text{O}_3-\text{Al}_2\text{O}_3-\text{SiO}_2-\text{TiO}_2-\text{H}_2\text{O}-\text{CO}_2$. *J Petrol* 29:445–522
- Berndt J, Koepke J, Holtz F (2005) An experimental investigation of the influence of water and oxygen fugacity on differentiation of MORB at 200 MPa. *J Petrol* 46:135–167
- Blewett DT, Robinson MS, Denevi BW, Gillis-Davis JJ, Head JW, Solomon SC, Holsclaw GM, McClintock WE (2009) Multispectral images of Mercury from the first MESSENGER flyby: Analysis of global and regional color trends. *Earth Planet Sci Lett* 285:272–282
- Boettcher AL, Burnham CW, Windom KE, Bohlen SR (1982) Liquids, glasses and the melting of silicates to high pressures. *J Geol* 90:127–138
- Bottinga Y, Weill DF (1972) The viscosity of magmatic silicate liquids: a model calculation. *Am J Sci* 272:438–475
- Bowen NL (1913) The melting phenomena of the plagioclase feldspars. *Am J Sci* 35:577–599
- Brugger CR, Johnston AD, Cashman KV (2003) Phase relations in silicic systems at one-atmosphere pressure. *Contrib Mineral Petrol* 146:356–369
- Burnham CW (1981) The nature of multicomponent aluminosilicate melts. *Phys Chem Earth* 13:197–226
- Carmichael IS (1964) The petrology of the Thingmuli Volcano in Eastern Iceland. *J Petrol* 5:435–460
- Carpenter MA (1988) Thermochemistry of aluminium/silicon ordering in feldspar minerals. In: Salje E (ed) *Physical properties and thermodynamic behaviour of minerals*. Dordrecht, Holland, pp 265–314
- Carpenter MA, McConnell JD (1984) Experimental delineation of the $\text{C1} = \text{I1}$ transformation in intermediate plagioclase feldspars. *Am Mineral* 69:112–121
- Courtial P, Gottsmann J, Holzheid A, Dingwell DB (1999) Partial molar volumes of NiO and CoO liquids: Implications for the pressure dependence of metal-silicate partitioning. *Earth Planet Sci Lett* 171:171–183
- Danyushevsky LV, Carroll MR, Falloon TJ (1997) Origin of high-An plagioclase in Tongan high-Ca boninites: implications for plagioclase-melt equilibria at low $p(\text{H}_2\text{O})$. *Can Min* 35:313–326
- Dijkstra AH, Drury MR, Vissers RL (2001) Structural petrology of plagioclase peridotites in the West Othris Mountains (Greece): melt impregnation in mantle lithosphere. *J Petrol* 42:5–24
- Elkins LT, Grove TL (1990) Ternary feldspar experiments and thermodynamic models. *Am Mineral* 75:544–559
- Feig S, Koepke JR, Snow J (2006) Effect of water on tholeiitic basalt phase equilibria: an experimental study under oxidizing conditions. *Contrib Mineral Petrol* 152:611–638
- Feig ST, Koepke J, Snow JE (2010) Effect of oxygen fugacity and water on phase equilibria of a hydrous tholeiitic basalt. *Contrib Mineral Petrol* 160:551–568
- Fram MS, Longhi J (1992) Phase equilibria of dikes associated with Proterozoic anorthosite complexes. *Am Mineral* 77:605–616
- Ghiorso MS, Sack RO (1995) Chemical mass transfer in magmatic processes. IV. A revised and internally consistent thermodynamic model for the interpolation and extrapolation of liquid-solid equilibria in magmatic systems at elevated temperatures and pressures. *Contrib Mineral Petrol* 119:197–212
- Ghiorso MS, Carmichael IS, Rivers ML, Sack RO (1983) The Gibbs free energy of mixing of natural silicate liquids: an expanded regular solution approximation for the calculation of magmatic intensive variables. *Contrib Mineral Petrol* 84:107–145
- Ghiorso MS, Hirschmann MM, Reiners PW, Kress VC (2002) The pMelts: a revision of Melts for improved calculation of phase relations and major element partitioning related to partial melting of the mantle to 3 GPa. *Geochem Geophys Geosyst* 3:1–36
- Glazner AF (1984) Activities of olivine and plagioclase components in silicate melts and their application to geothermometry. *Contrib Mineral Petrol* 88:260–268
- Grove TL, Bryan WB (1983) Fractionation of pyroxene-phyric MORB at low pressure: an experimental study. *Contrib Mineral Petrol* 84:293–309
- Grove TL, Gerlach DC, Sando TW (1982) Origin of calc-alkaline series lavas at Medicine Lake Volcano by fractionation, assimilation and mixing. *Contrib Mineral Petrol* 80:160–182
- Grove TL, Kinzler RJ, Bryan WB (1992) Fractionation of mid-ocean ridge basalt (MORB). In: Phipps-Morgan J, Blackman DK, Sinton JM (eds) *Mantle flow and melt generation at mid-ocean ridges*. Am Geophys Union pp 281–310
- Hamada M, Fuji T (2007) H_2O -rich island arc low-K tholeiite magma inferred from Ca-rich plagioclase-melt inclusion equilibria. *Geochem J* 41:437–461
- Hawke BR, Peterson CA, Blewett DT, Bussey DB, Lucey PG, Taylor GJ, Spudis PD (2003) Distribution and modes of occurrence of lunar anorthosite. *J Geophys Res* 108:5050
- Henry DJ, Navrotsky A, Zimmermann HD (1982) Thermodynamics of plagioclase-melt equilibria in the system albite-anorthite-diopside. *Geochim Cosmochim Acta* 46:381–391
- Hess PC (1977) Structure of silicate melts. *Can Min* 15:162–178
- Holland T, Powell R (1992) Plagioclase feldspars: activity-composition relations based upon Darken's quadratic formalism and Landau theory. *Am Mineral* 77:53–61
- Holzheid A, Grove TL (2005) The effect of metal composition on Fe-Ni partition behavior between olivine and FeNi-metal, FeNi-carbide, FeNi-sulfide at elevated pressure. *Chem Geol* 221:207–224
- Holzheid A, Palme H, Chakraborty S (1997) The activities of NiO, CoO and FeO in silicate melts. *Chem Geol* 139:21–38
- Housh TB, Luhr JF (1991) Plagioclase-melt equilibria in hydrous systems. *Am Mineral* 76:477–492
- Karner J, Papike JJ, Shearer CK (2004) Plagioclase from planetary basalts: chemical signatures that reflect planetary volatile budgets, oxygen fugacity, and styles of igneous differentiation. *Am Mineral* 89:1101–1109
- Kerrick DM, Darken LS (1975) Statistical thermodynamic models for ideal oxide and silicate solid solutions, with application to plagioclase. *Geochim Cosmochim Acta* 39:1341–1442
- Kudo AM, Weill DF (1970) An igneous plagioclase thermometer. *Contrib Mineral Petrol* 25:52–65
- Lange RA (2003) The fusion curve of albite revisited and the compressibility of $\text{NaAlSi}_3\text{O}_8$ liquid with pressure. *Am Mineral* 88:109–120
- Lange RA, Frey HM, Hector J (2009) A thermodynamic model for the plagioclase-liquid hygrometer/thermometer. *Am Mineral* 94:494–506
- Le Maitre RW (1989) A classification of igneous rocks and glossary of terms: recommendations of the International Union of

- Geological Sciences. Subcommittee on systematics of igneous rocks. Blackwell, Oxford, p 193
- Libourel G (1999) Systematics of calcium partitioning between olivine and silicate melt: Implications for melt structure and calcium content of magmatic olivines. *Contrib Mineral Petrol* 136:63–80
- Libourel G, Boivin P, Biggar GM (1989) The univariant curve liquid = forsterite + anorthite + diopside in the system CMAS at 1 bar: solid solutions and melt structure. *Contrib Mineral Petrol* 102:406–421
- Lindsley DH (1970) Melting relations of plagioclase at high pressures. New York State Museum and Science Service Memoir 18:39–46
- Longhi J, Fram MS, Vander Auwera J, Montieth JN (1993) Pressure effects, kinetics, and rheology of anorthositic and related magmas. *Am Mineral* 78:1016–1030
- Mathez EA (1973) Refinement of the Kudo-Weill plagioclase thermometer and its application to basaltic rocks. *Contrib Mineral Petrol* 41:61–72
- Mathieu (2009) Solubilité du sodium dans les silicates fondus. Ph.D. Thesis, Institut National Polytechnique de Lorraine, France: 393p
- Mysen BO (1990) Relationships between silicate melt structure and petrologic processes. *Earth Sci Rev* 27:281–365
- Mysen BO, Richet P (2005) Silicate melts: properties and structure. Elsevier, Amsterdam, p 544p
- Ohtake M, Matsunaga T, Haruyama J, Yokota Y, Morota T, Honda C, Ogawa Y, Torii M, Miyamoto H, Arai T, Hirata N, Iwasaki A, Nakamura R, Hiroi T, Sugihara T, Takeda H, Otake H, Pieters CM, Saiki K, Kitazato K, Abe M, Asada N, Demura H, Yamaguchi Y, Sasaki S, Kodama S, Terazono J, Shirao M, Yamaji A, Minami S, Akiyama H, Josset J-L (2009) The global distribution of pure anorthosite on the Moon. *Nature* 461:236–240
- Orville PM (1972) Plagioclase cation exchange equilibria with aqueous chloride solution: results at 700°C and 200 bars in the presence of quartz. *Am J Sci* 272:234–272
- Panjasawatwong Y, Danyushevsky LV, Crawford AJ, Harris KL (1995) An experimental study of the effects of melt composition on plagioclase-melt equilibria at 5 and 10 kbar: Implications for the origin of magmatic high-An plagioclase. *Contrib Mineral Petrol* 118:420–432
- Powell R (1987) Darken's quadratic formalism and the thermodynamics of minerals. *Am Mineral* 72:1–11
- Price JG (1985) Ideal site mixing in solid solutions, with an application to two-feldspars geothermometry. *Am Mineral* 70:696–701
- Putirka KD (1999) Clinopyroxene + liquid equilibria to 100 kbar and 2450 K. *Contrib Mineral Petrol* 135:151–163
- Putirka KD (2005) Igneous thermometers and barometers based on plagioclase + liquid equilibria: Tests of some existing models and new calibrations. *Am Mineral* 90:336–346
- Putirka KD, Mikaelian H, Ryerson F, Shaw H (2003) New clinopyroxene-liquid thermobarometers for mafic, evolved, and volatile-bearing lava compositions, with applications to lavas from Tibet and the Snake River Plain, Idaho. *Am Mineral* 88:1542–1554
- Rao MN, Borg LE, McKay DS, Wentworth SJ (1999) Martian soil component in impact glasses in a Martian meteorite. *Geophys Res Lett* 26:3265–3268
- Renne PR (2000) $^{40}\text{Ar}/^{39}\text{Ar}$ age of plagioclase from Acapulco meteorite and the problem of systematic errors in cosmochronology. *Earth Planet Sci Lett* 175:13–26
- Richet P, Bottinga Y (1984a) Glass transitions and thermodynamic properties of amorphous SiO_2 , $\text{NaAlSi}_n\text{O}_{2n+2}$ and KAlSi_3O_8 . *Geochim Cosmochim Acta* 48:453–470
- Richet P, Bottinga Y (1984b) Anorthite, andesine, wollastonite, diopside, cordierite and pyrope: thermodynamics of melting, glass transitions, and properties of the amorphous phases. *Earth Planet Sci Lett* 67:415–432
- Righter K, Drake MJ (1997) A magma ocean on Vesta: core formation and petrogenesis of eucrites and diogenites. *Meteor Planet Sci* 32:929–944
- Shearer CK, Hess PC, Wieczorek MA, Pritchard ME, Borg LE, Longhi J, Elkins LT, Neal CR, Antonenko I, Canup RM, Halliday AN, Grove TL, Hager BH, Lee DC, Wiechert U (2006) Thermal and magmatic evolution of the moon. *Rev Mineral Geochem* 60:365–518
- Shi P (1993) Low-pressure phase relationships in the system $\text{Na}_2\text{O}-\text{CaO}-\text{FeO}-\text{MgO}-\text{Al}_2\text{O}_3-\text{SiO}_2$ at 1,100°C, with implications for the differentiation of basaltic magmas. *J Petrol* 34:743–762
- Shi P, Libourel G (1991) The effects of FeO on the system CMAS at low pressure and implications for basalt crystallization processes. *Contrib Mineral Petrol* 108:129–145
- Sisson TW, Grove TL (1993) Experimental investigations of the role of H_2O in calc-alkaline differentiation and subduction zone magmatism. *Contrib Mineral Petrol* 113:143–166
- Stebbins JF, Weill DF, Carmichael IS, Moret LS (1982) High temperature heat contents and heat capacities of liquids and glasses in the system $\text{NaAlSi}_3\text{O}_8-\text{CaAl}_2\text{Si}_2\text{O}_8$. *Contrib Mineral Petrol* 80:226–244
- Stormer JC, Nicholls J (1978) XLFAC: a program for the interactive testing of magmatic differentiation models. *Comput Geosci* 4:143–159
- Takagi D, Sato H, Nakagawa M (2005) Experimental study of a low-alkali tholeiite at 1–5 kbar: optimal condition for the crystallization of high-an plagioclase in hydrous arc tholeiite. *Contrib Mineral Petrol* 149:527–540
- Taylor GJ (2009) Ancient lunar crust: Origin, composition and implications. *Elements* 5:17–22
- Tenner TJ, Lange RA, Downs RT (2007) The albite fusion curve re-examined: new experiments and the high-pressure density and compressibility of high-albite and $\text{NaAlSi}_3\text{O}_8$ liquid. *Am Mineral* 92:1573–1585
- Thy P, Leshner CE, Tegner C (2009) The Skaergaard liquid line of descent revisited. *Contrib Mineral Petrol* 157:735–747
- Toplis MJ (2005) The thermodynamics of iron and magnesium partitioning between olivine and liquid: Criteria for assessing and predicting equilibrium in natural and experimental systems. *Contrib Mineral Petrol* 149:22–39
- Toplis MJ, Carroll MR (1995) An experimental study of the influence of oxygen fugacity on Fe-Ti oxide stability, phase relations, and mineral-melt equilibria in ferro-basaltic systems. *J Petrol* 36:1137–1170
- Toplis MJ, Carroll MR (1996) Differentiation of ferro-basaltic magmas under conditions closed and open to oxygen: implications for the Skaergaard intrusion and other natural systems. *J Petrol* 37:837–858
- Weaver JS, Langmuir CH (1990) Calculation of phase equilibrium in mineral-melt systems. *Comput Geosci* 16:1–19
- Wood JA, Dickey JS, Marvin UB, Powell BN (1970) Lunar anorthosites. *Science* 167:602–604